Cement and Concrete Research 58 (2014) 35–44

Contents lists available at ScienceDirect

Cement and Concrete Research

journal homepage: http://ees.elsevier.com/CEMCON/default.asp

Simulation of the capillary flow of an autonomic healing agent in discrete cracks in cementitious materials ☆

Diane Gardner *, Anthony Jefferson [1], Andrea Hoffman [1], Robert Lark [1]

School Office, Cardiff School of Engineering, Queen's Buildings, The Parade, Newport Road, Cardiff CF24 3AA, United Kingdom

ARTICLE INFO

Article history:
Received 18 December 2012
Accepted 6 January 2014
Available online xxxx

Keywords:
Healing agents
Transport properties (C)
Modelling (E)
Mortar (E)

ABSTRACT

Autonomic self-healing cementitious materials generally rely upon the transport of adhesives via capillary flow in discrete cracks to heal macro-cracks. A series of experimental and numerical studies are presented that simulate the capillary flow of cyanoacrylate in a range of discrete cracks in prismatic cementitious specimens. The numerical procedure developed incorporates corrections to established capillary flow theory to consider stick-slip behaviour of the meniscus and frictional dissipation at the meniscus wall boundary. In addition, two short benchmark studies are reported in order to firstly verify the time–viscosity relationship of the cyanoacrylate in a mortar capillary channel and secondly to examine the capillary flow of the healing agent in small diameter glass capillaries. These studies also provide data to validate the numerical model. The capillary rise response of a healing agent in a self-healing system is predicted using the calibrated model and verified with published experimental data.

1. Introduction and literature review

In the last decade considerable research effort has been directed towards the development of self-healing materials in order to overcome the construction industry wide problem of civil infrastructure deterioration. These self-healing materials have the ability to adapt and respond to environmental and operational changes to which they may be subjected [1,2]. Such materials are generally classified as 'smart' materials and include self-healing materials as a particular sub-set [3]. In the case of concrete, the presence of pores and cracks in the matrix, the latter caused as a result of plastic shrinkage, mechanical loading and thermal effects amongst other actions, allows the movement of water and gases that contribute to the deterioration of a structure. However, networks of connected pores and cracks may also provide pathways for the flow of healing agents.

Two types of self-healing in cementitious materials are referred to in the literature. The first is autogenic healing, a natural phenomenon which occurs mainly due to the pozzolanic properties of cementitious materials [4–7]. The second type of healing is termed autonomic healing and is a concept originally proposed in 1994 for cementitious materials by Dry [8]. These self-healing cementitious materials normally have tubes or capsules of adhesive agents embedded within the cementitious matrix that, upon damage, break and release the agent into the matrix. The adhesive then flows under capillary action to macro-cracked and micro-cracked regions. The methods of encapsulation have included discrete microcapsules [9], continuous hollow lengths of glass [10,11] and ceramic capillary tubes [12]. Although the concept of autonomic healing has been proven using these techniques at a small scale, there is still significant research required to select an appropriate encapsulation system which can withstand the rigours of reinforcement placement and concrete casting [3].

Alkali–silica and sodium silicate solutions [9,13], one- and two-component epoxy resins [9,14], cyanoacrylates [10,11] and most recently a two-component expanding polyurethane foam [12] have been used as healing agents with varied success. The selection of healing agents is usually based on a number of requirements; the agent must have a sufficiently low viscosity to flow into and around the damage region; it must have the ability to bond together two faces and it should have a sufficient shelf life to allow encapsulation for long periods of time without deterioration of the bonding properties [11]. The ability to guarantee the availability and subsequent adequate mixing of both parts of a two-component healing agent at a crack location may be limited [12] and therefore one-component systems may offer significant advantages in this respect.

Cyanoacrylates, more commonly referred to as superglues, typically have a shelf life of one year. When encapsulated within concrete they would be expected to heal damage that occurs within the early life of a structure, due to early thermal effects, shrinkage and construction loading. However, the future development of flow networks may offer the potential to continually deliver superglues and resins to zones of damage throughout the working life of a structure thereby removing the constraint of the healing agent's shelf life.

Previous experiments undertaken on self-healing cementitious materials have established that agents will flow under capillary action

* Corresponding author. Tel.: +44 29 2087 0776; fax: +44 29 2087 4939.
E-mail addresses: Gardnerdr@cf.ac.uk (D. Gardner), Jeffersonad@cf.ac.uk (A. Jefferson), Lark@cf.ac.uk (R. Lark).
[1] Tel.: +44 29 2087 0776; fax: +44 29 2087 4939.

0008-8846/$ – see front matter © 2014 The Authors. Published by Elsevier Ltd. All rights reserved.
http://dx.doi.org/10.1016/j.cemconres.2014.01.005

Table 1
Capillary rise theory.

$2\pi r\gamma\cos(\theta)-\pi r^2\rho g z\sin(\varphi)-8\pi\mu z\dot{z}-\rho\pi r^2\frac{\partial}{\partial t}(z\dot{z})=0$ (1)	Full dynamic flow equation for of liquid in a capillary tube (Lucas–Washburn (L–W) equation).
$p_c-\rho g z\sin(\varphi)-\frac{\mu}{k}z\dot{z}=0$ (2)	L–W equation without inertial and gravitational effects.
$p_c=\frac{2\gamma\cos(\theta)}{r}$ (3)	Young–Laplace equation for capillary pressure.
$h_{eq}=\frac{p_c}{\rho g\sin(\varphi)}$ (4)	Equilibrium capillary liquid rise height from balance of hydrostatic and capillary pressure.
$\beta_s=1-\frac{h_s}{h_{eq}}$ (5)	Correction factor for stick-slip behaviour of the meniscus (unitless) [18].
$\gamma\cos(\theta(t))=\gamma\cos(\theta_0)-\beta_m\dot{z}$ (6)	Correction factor for frictional dissipation at the moving front (units Ns/m^2) after [19,20].
$\dot{z}=\left(\frac{r\beta_w}{2}+\frac{r^2}{8\mu}\right)\left(\frac{p_c}{z}\right)$ (7)	Velocity of meniscus including the correction factor for wall slip (β_w units m^3/Ns) [21].
$p_{c0}(1-\beta_s)-\frac{2\beta_m\dot{z}}{r}-\rho g z\sin(\varphi)-\left(\frac{z}{\frac{r\beta_w}{2}+\frac{r^2}{8\mu}}\right)\dot{z}=0$ (8)	Amended L–W equation proposed by Gardner et al. [16].

([11,12,15]), but to the authors' knowledge, no detailed investigation has been undertaken on the capillary flow of healing agents in cracks in cementitious materials. It is expected that the quantity and rate of flow will be governed by the profile and nature of the crack, the curing rate of the agent as well as by chemical interactions between the host matrix and the healing agent, which may affect this curing rate. The quantification and simulation of this flow is the subject of the present publication. The ability to measure and predict the capillary flow of healing agents through cracks in cementitious materials will allow more efficient self-healing systems to be designed in the future.

This paper presents experimental data on the capillary flow of cyanoacrylate, an all purpose superglue, in discrete cracks in cementitious materials obtained via high speed video measurement. The paper also considers the capillary flow of a cyanoacrylate in a self-healing system and introduces a numerical model to simulate experimentally observed results. The structure of the paper is as follows:

- Section 2 provides an overview of standard Lucas–Washburn capillary flow theory as well as the amendments explored by Gardner et al. [16] and develops this theory further to consider flow in a discrete crack of varying aperture.
- Section 3 presents details of a study performed to provide an independent verification of the viscosity of the cyanoacrylate adhesive and an indication of its time–viscosity behaviour over a 15 minute timescale.
- Section 4 employs the amended theory to simulate the experimentally observed flow of cyanoacrylate in a glass capillary tube.
- Section 5 presents the experimental data on the flow of cyanoacrylate in openings in cementitious materials; including data from experiments with planar, inclined and tapered apertures or 'cracks'. It also provides a comparison between the amended flow theory and the experimental data presented.
- Finally, in Section 6, a study is described which ascertains whether the flow of cyanoacrylate in a natural discrete crack in the self-healing system proposed by Joseph et al. [11] can be predicted using the amended theory.

The present investigation concentrates on the flow of cyanoacrylate in a discrete crack with no detailed consideration being given to flow into or out of the porous media adjacent to the discrete opening. The importance of including both aspects of flow behaviour when simulating these problems with, for example, a finite element model, is however fully acknowledged [17] and this issue is the subject of on-going work.

2. Capillary rise theory

The capillary flow theory previously presented by Gardner et al. [16] is summarised in Table 1. The omission of the inertial term in the consideration of water flow in a capillary tube has been justified previously by Gardner et al. [16] and it is considered that the relative importance of inertia term will be even less for cyanoacrylate, which has a higher viscosity than water.

Where:

- z = capillary rise height (m); γ = surface tension (N/m); θ = liquid/solid contact angle (°); φ = capillary inclination angle (°); ρ is the density of liquid (kg/m^3); g = gravitational acceleration (m/s^2); r = radius of the capillary (m); μ = dynamic viscosity (Ns/m^2); t = capillary rise time (s); effective permeability term $k = r^2/8$ [22];
- h_s = the rise height allowing for pinning (modified capillary rise height);
- $p_{c0}=\frac{2\gamma\cos(\theta_0-\alpha)}{r}$ where θ_0 is the static contact angle (°) and α is the inclination of the capillary wall (°).

In an earlier study, Gardner et al. [16] reported no significant influence of wall slip (β_w term) on the capillary rise response of water in glass capillary tubes or discrete cracks in mortar, however, this term is shown here for completeness.

Young [22] accounted for a change in fluid velocity as a result of non-uniform capillaries (Fig. 1) by applying the mass balance equation (9) to the L–W Eq. (1):

$$\dot{z}A(z)=v(x)A(x) \tag{9}$$

Applying the same principles to Eq. (8) leads to the following equation for flow in non-uniform capillaries which allows for stick slip and frictional dissipation.

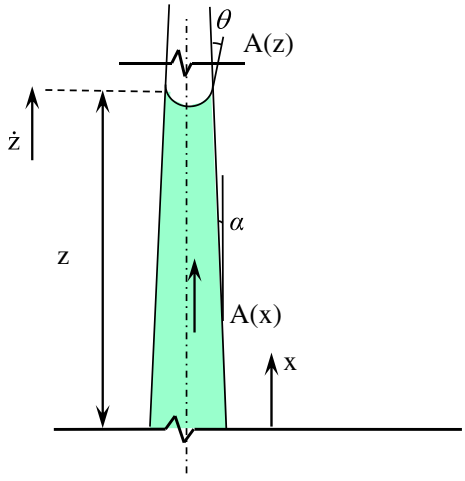

Fig. 1. Illustration of the parameters used to model water flow in a non-uniform capillary.

$$\dot{z} = \frac{p_{c0}(1-\beta_s) - \rho g z \sin(\varphi)}{\frac{2\beta_m}{r(z)} + \eta} \tag{10}$$

and in which

$$\eta = A(z)\int_0^z \frac{1}{\left(\frac{r(x)\beta_w}{2} + \frac{k(x)}{\mu}\right)A(x)}dx \tag{11}$$

It is noted that the term η represents the total viscous resistance to flow (per unit area at the meniscus) and has the units Ns/m^3.

Eq. (10) is solved using a direct integration time-stepping procedure. A check is undertaken to ensure that the time step is sufficiently small to give converged results.

A similar numerical solution has been developed in this work for planar cracks in cementitious materials, whereby the radius of the capillary tube, r, is replaced by the crack width, b and the effective permeability term takes the value $k = b^2/12$ [23].

The influence of the three correction parameters on the capillary rise response of cyanoacrylate ($\theta = 90^o$; $\rho = 1060\ kg/m^3$; $\mu = 0.004\ Ns/m^2$) in a 0.5 mm diameter capillary and in a 1 mm to 0.1 mm tapering crack (i.e. planar opening) is shown in Fig. 2 (a) and (b) respectively. The capillary rise results in a capillary tube are compared to predictions made using the analytical solution proposed by Fries and Dreyer [24]. The results are normalised by considering h_{eq}, the equilibrium rise height as calculated in Eq. (4), and t*, the time taken to reach 99% of h_{eq} if all correction factors are set to zero. For flow in a tapering crack, a numerical solution was used to obtain the results and for this case h_{eq} was taken as the final rise height obtained with all β correction factors set to zero. This procedure allows the influence of each correction factor on the response curve to be observed. It may be seen in Fig. 2 that β_s causes a decrease in both the final rise height and the rise rate. It can also be observed that the inclusion of the β_m correction factor retards the capillary rise response whilst the β_w correction factor accelerates the capillary rise response of the system as a result of the decreased net resistance to flow.

In this work the above theory has been applied to planar and tapering cracks, however it can in principle describe the capillary flow in a discrete crack of any (2D) configuration, since the governing equation allows for varying aperture and inclination. In the present implementation, cracks are divided into piece-wise sections of constant inclination and linearly varying aperture. Thus, if the characteristic dimensions of a rough crack were available the model could be used with multiple segments to represent the capillary flow. However, such data are rarely available and the authors therefore derived a method for determining the properties of planar crack which have essentially the same flow characteristics as a natural crack of known average opening [16]. Furthermore, work is in progress to include a sink-source term in the mass continuity equation to allow for the flow of healing agent into the micro-cracked zone adjacent macro-crack and to link the discrete crack flow model to a continuum finite element model of the porous cementitious media.

3. Investigation of time dependent properties of cyanoacrylate

Cyanoacrylates are acidic solutions which have the ability to bond gaps of 0.05 mm and smaller within two seconds [25] however, Joseph et al. [11] suggested that the conditions within the mortar, including the highly alkaline environment and the presence of moisture, further accelerate the curing process of cyanoacrylate. In order to provide an independent verification of the viscosity of the cyanoacrylate and its curing behaviour during the capillary rise simulations, a series of bespoke tests, based on the principle of the Ostwald viscometer, were performed.

Two sets of flow tests were conducted in which a central constricted channel was connected to two L-shaped channels formed from flexible tubing. In the first set of these tests, the central channel section was a section of glass capillary tube as illustrated in Fig. 3 (a) and in the second set the central channel section was formed by drilling a circular hole through a mortar prism as illustrated in Fig. 3 (b).

The channels were cleaned with pressurised air and then filled with a single-agent cyanoacrylate adhesive (Procure PC20), supplied by Cyanotech Ltd. One end of the channel was raised and a stopper placed in the flexible tube. The channel was then returned to the horizontal position and the stopper removed. The movement of the cyanoacrylate free surface (i.e. dh_1/dt) was recorded using a high speed video camera. The test was initially repeated at 10 second intervals and this was gradually increased to 5 minute intervals over a period of 15 min. Additionally, the at rest level of the cyanoacrylate was recorded after each test to measure any losses which may have occurred due to either hardening of the adhesive or absorption into the matrix surrounding the capillary bore. It is noted that no significant losses were measured during the course of these tests.

It was observed that, in one of the mortar specimen tests, a "skin" had formed on the cyanoacrylate surface 90 min after commencement of the test, and that after this time no flow of cyanoacrylate could be induced. By contrast, the cyanoacrylate in the glass channel showed no evidence of curing or hardening over a period of 72 h after commencement of the test. The experimental results from the tests are presented in Fig. 4.

In order to obtain an analytical expression for the displacement of the free surface of the cyanoacrylate in the experimental arrangement presented in Fig. 3, the momentum balance of the liquid inside a tube is considered. The following assumptions are made: i) the flow is one dimensional (i.e. no variation of flow velocity across the pipe cross-

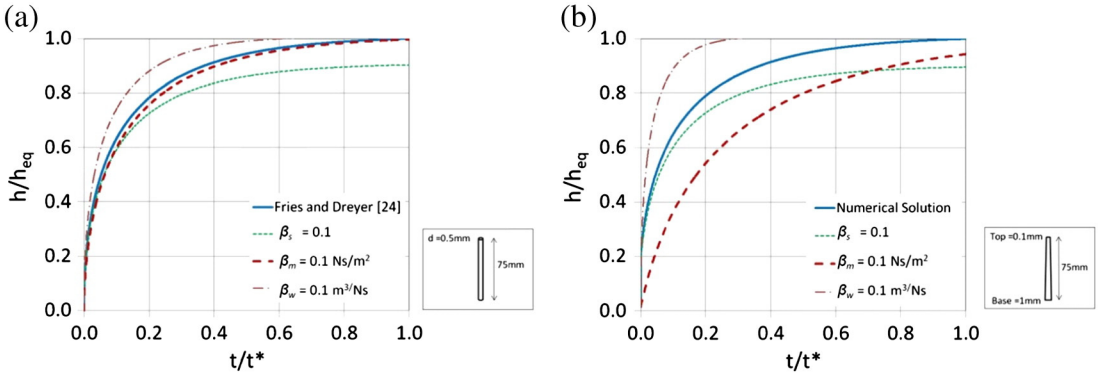

Fig. 2. The effect of correction parameters on capillary rise response for 2 different experimental arrangements: (a) Capillary diameter of 0.5 mm and (b) Tapering 1 mm to 0.1 mm crack.

Test	Channel	r_1 (mm)	r_2 (mm)	r_2 (mm)	L_1 (mm)	L_2 (mm)	L_3 (mm)	$\bar{h}$ (mm)
G1	Glass	2.0	1.3	2.0	87.5	58	87.5	0.060
M1	Mortar	2.5	2.1	2.5	57.5	52	57.5	0.0125

r_i= radius of section i A_i = cross-sectional area for section i

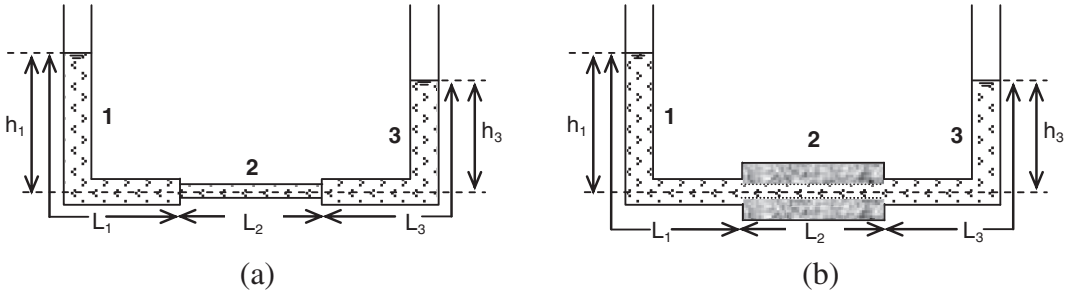

Fig. 3. Viscosity test experimental arrangement: (a) central glass channel and (b) central drilled channel in mortar.

section is considered), ii) mass continuity is maintained, with no fluid losses considered, iii) any forces from displaced air are negligible, iv) no energy losses occur at the junctions between two channel sections, and v) the pressure gradient is related to the viscous resistance by the Hagen–Poiseuille equation. With these assumptions, the momentum balance of a liquid inside a capillary tube may be written:

$$\rho g(h_1-h_3)A_1-8\mu\sum_{i=1}^{3}A_i\frac{L_i u_i}{r_i^2}-\rho\sum_{i=1}^{3}A_i L_i u_i=0, \tag{12}$$

where u_i is the flow velocity of channel i (i designating the flexible tube, capillary channel or channel in the mortar), and the superior dot denotes the time derivative. Mass continuity of the fluid implies that $u_i=-\dot{h}_i$, $\bar{h}=\frac{h_1+h_3}{2}$ and $A_i u_i = const.$ Applying these conditions in Eq. (12) and rearranging gives the following governing differential equation:

$$\ddot{h}_1+\frac{K_{HP}}{\rho L_T}\dot{h}_1+\frac{2g}{L_T}h_1=\frac{2g}{L_T}\bar{h}, \tag{13}$$

in which $K_{HP}=8\mu\sum_{i=1}^{3}\frac{L_i}{r_i^2}$ and $L_T=\sum_{i=1}^{3}L_i$.

The solution of Eq. (13) is given below but it is noted that this is only valid if the discriminant of the associated characteristic equation is negative, i.e. the roots are complex.

The initial conditions used in the solution to derive Eq. (14) are as follows:

$h_1=h_{10}$ and $\dot{h}_1=\dot{h}_{10}@t=0$.

Application of these conditions leads to the following equation:

$$h_1=e^{\lambda t}\left[\left(h_{10}-\bar{h}\right)\cos\chi t+\left(\frac{\dot{h}_{10}-\lambda\left(h_{10}-\bar{h}\right)}{\chi}\right)\sin\chi t\right]+\bar{h} \tag{14}$$

in which

$$\lambda=-\left(\frac{K_{HP}}{2\rho L_T}\right) \text{ and } \chi=\sqrt{\frac{2g}{L_T}-\left(\frac{K_{HP}}{2\rho L_T}\right)^2}.$$

The viscosities for the two cases considered (i.e. for each time and configuration) were computed by using a least squares fit of Eq. (14) to the associated experimental data and were 0.00423 Ns/m^2 and 0.00366 Ns/m^2 for tests G1 and M1 respectively. This is in good agreement with the technical data provided by the manufacturer [25] which suggests a typical viscosity of 0.004 Ns/m^2. The numerical simulations of the experimental arrangement using these viscosities are presented in Fig. 4. After 15 min, the viscosity remained unchanged, although potential contamination of the cyanoacrylate by the mortar may have been responsible for the complete hardening of the

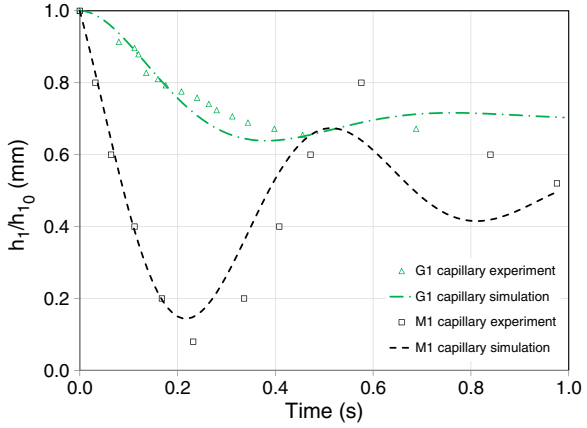

Fig. 4. Comparison of experimental data and numerical simulations for G1 and M1 tests using viscosities calculated using a least squares fit to Eq. (14).

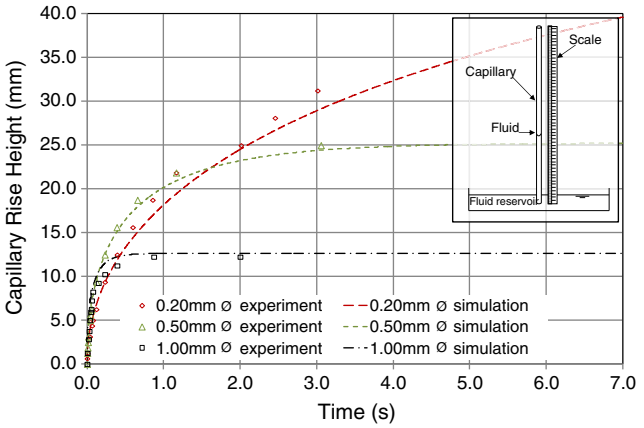

Fig. 5. Comparison of experimental data and numerical simulation of the capillary rise of cyanoacrylate in borosilicate glass tubes, $\beta_s=0.01$, $\beta_m=0.08$ Ns/m^2, $\beta_w=0$ m^3/Ns.

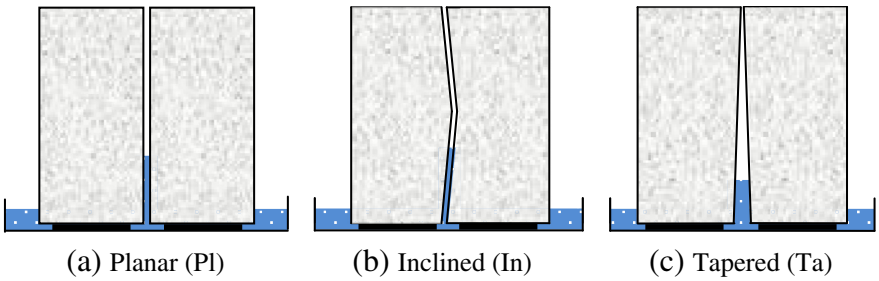

Fig. 6. Schematic representation of crack configurations.

cyanoacrylate in the flexible tubes in the subsequent hours after the first contact of cyanoacrylate with the mortar. It is noted that the abscissa in Fig. 4 is the time from the start of the first test of the series presented.

4. Investigation of capillary rise behaviour of cyanoacrylate in glass capillary tubes

Experimental validations of the capillary flow theory were performed as part of this study using borosilicate glass tubes supplied by CM Scientific Ltd., as presented in Fig. 5. These tubes were used in a nominally 'as supplied' clean condition and were not subjected to any additional cleaning or wetting prior to testing. Capillary tubes of 0.2 mm and 1.0 mm diameters were tested.

For the experiments conducted, the correction factors required to provide a close match with the experimental data for both capillary tubes were $\beta_s = 0.01$, $\beta_m = 0.08$ Ns/m^2 and $\beta_w = 0$ m^3/Ns, based on the numerical solution of Eq. (10). There was no evidence of curing of the cyanoacrylate during the tests and this observation is supported by the free movement of the cyanoacrylate column in the capillary tube during agitation of the tube in the subsequent minutes after each capillary rise test.

The contact angle between the glass capillary tube and the cyanoacrylate liquid surface was measured as 10° using an optical microscope. Values for surface tension and density were taken from the cyanoacrylate data sheet [25] and were 0.033 N/m and 1060 kg/m^3 respectively.

5. Investigation of capillary rise behaviour in cementitious materials

The general arrangement of the capillary rise tests in cracks within mortar specimens are shown in Fig. 6.

5.1. Materials and mix proportions

A mortar, with an average compressive strength of 37 N/mm^2, was used throughout the study. Cement type CEM II/B-V 32,5R conforming to BS EN 197-1:2000, together with a marine dredged sand, with a maximum particle size of 2 mm, were employed in the mix in the following proportion — 540 kg/m^3:1618 kg/m^3:242 kg/m^3 (cement:sand:water).

5.2. Specimen preparation and capillary rise simulations

The experimental studies were performed on mortar specimens after 7 days and 28 days of curing. In the former, the specimens were demoulded and left to air cure until the testing date. In the latter, the specimens were demoulded and the prisms were wrapped in damp hessian for 14 days and then left to air cure at a temperature of 21 °C for a further 14 days. Prisms of size 75 mm × 75 mm × 255 mm were cast and planar (Pl) and tapered (Ta) openings were formed by wet cutting each prism into seven pairs of 30 mm × 30 mm × 75 mm specimens using a circular saw. The specimens were then left to dry in the laboratory environment for a further week prior to testing. Inclined (In) cracks were formed using a series of folded plates of 2 mm

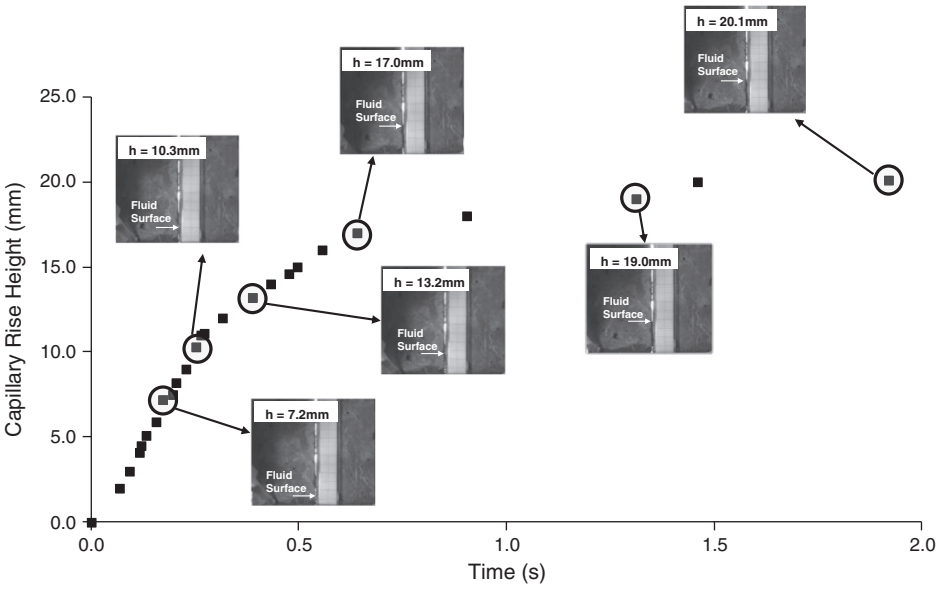

Fig. 7. Example of video image data for the capillary rise response of 7-Pl-0.271.

thickness placed vertically in the prismatic moulds, before being cut in the same manner as the planar crack specimens. These plates were manufactured so that the angle of the flow path deviated from the vertical by ± 5°. Both planar and inclined crack surfaces were filed with a fine glass paper and cleaned with pressurised air prior to testing. A schematic representation of the crack configurations is given in Fig. 6.

For each crack type, a series of crack apertures were achieved by using spacers which comprised short lengths of wires with diameters varying from 0.094 to 0.900 mm. The wires were placed between a pair of mortar specimens and the pair of specimens clamped together. These short wire spacers were placed near the edges of the specimens and are considered too small to have significantly interrupted the overall capillary flow.

A series of measurements of the crack aperture at the surface were taken using a Beck Luminex microscope. For the planar and inclined specimens a mean crack aperture was calculated based on these observations. For the tapered specimens the crack aperture was measured once at the base and once at the top of the specimen. Planar and inclined test specimen designations were "age (days)-crack configuration-aperture (mm)", for example 28-Pl-0.502 represents a 28 day old specimen with a planar crack configuration of 0.502 mm aperture. For tapered specimens both the base and top apertures were included in the specimen designation.

The capillary rise response was captured with a high speed digital camera, as previously described in full by Gardner et al. [16]. The camera was mounted on a platform 300 mm in front of the specimens. A laminated scale was used to measure capillary rise and was adhered to one side of the crack on the front face of the specimens. During the recording phase of the experiment, adjustable lighting was used in front of and behind the specimens to enhance the visibility of the crack.

5.3. Experimental and numerical simulation of capillary rise

In this section, comparisons are made between a selection of the results from experiments described in Section 5.2 of this paper and the results obtained from the numerical model presented in Section 2. The experimental results presented examine the effect of crack aperture and crack configuration on the level and rate of capillary rise of cyanoacrylate. Moreover the effect of age is also considered in the context of planar and tapered cracks. Capillary rise responses were extracted

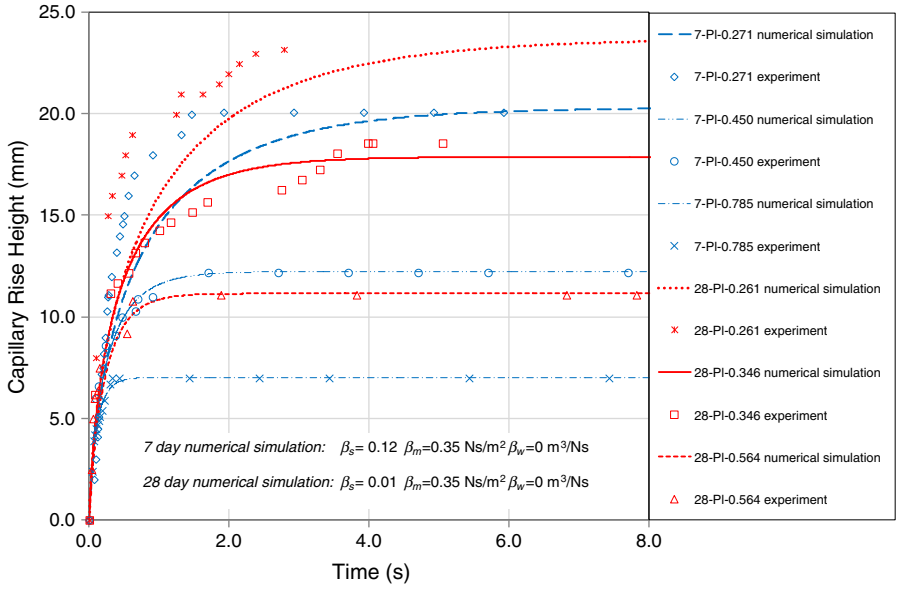

(a)

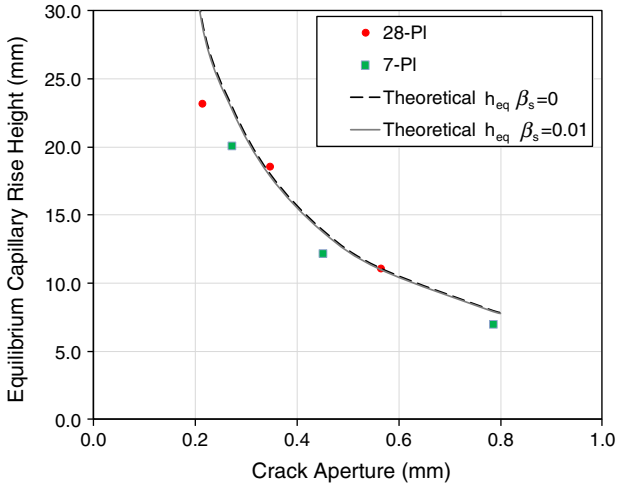

(b)

Fig. 8. (a) Planar Crack capillary rise response for 7 and 28 day old specimens. (b) Comparison with theoretical data.

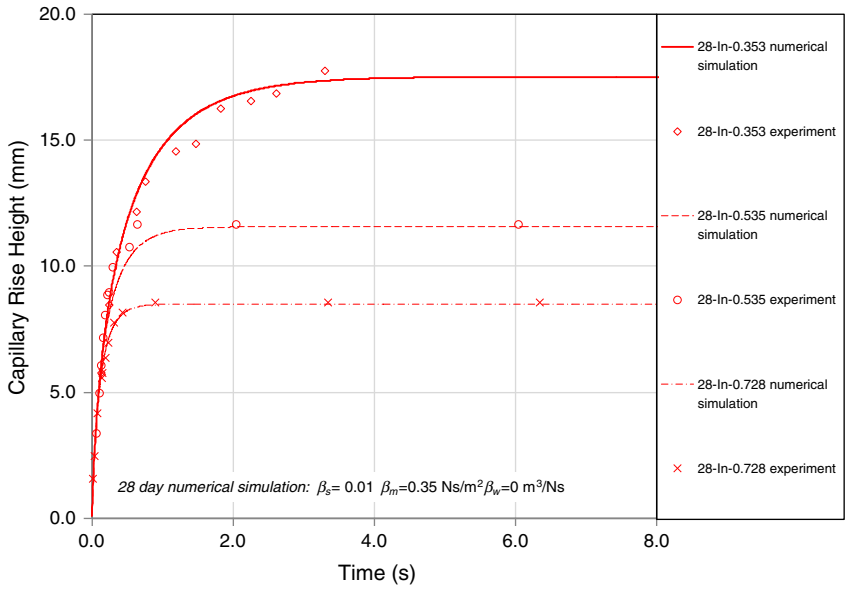

Fig. 9. Capillary rise height data at 28 days for inclined planar crack configuration.

from the video files, in a similar sequence to that illustrated in Fig. 7 which shows a typical capillary rise height response for a planar crack aperture of 0.271 mm together with the source data.

In order to simulate the capillary rise response for a planar crack aperture, the average (mean) crack aperture as measured in the experiment was used. For the tapering crack, the exact crack geometry was used in the numerical model. The viscosity used in the numerical simulations was 0.00366 Ns/m^2 as established for cyanoacrylate in mortar capillaries in Section 3 of this paper. On obtaining the equilibrium rise height, the β_s correction parameter was adjusted until the experimental rise height was achieved. The correction parameter β_m was then modified until the capillary rise response as observed in the experiment was reproduced.

Firstly the capillary rise response for a range of planar crack apertures are considered, the results of which are presented in Fig. 8 (a). The specimens under examination were in the laboratory dry state. For all crack apertures examined, the equilibrium capillary rise height is consistent with that predicted from capillary flow theory (Eqs. (4) and (5)), using a contact angle of 10° (as measured previously), a surface tension of cyanoacrylate of 0.033 N/m and a β_s correction parameter of 0.01, as shown in Fig. 8 (b).

The results show that β_s decreases from 0.12 for the 7 day old specimen to 0.01 for the 28 day specimen. This observed reduction in the stick slip parameter with mortar age is attributed to changes in the mortar microstructure due to continued hydration, with the surface to which the adhesive adheres gradually becoming drier and denser as hydration proceeds.

Experimental and numerical capillary rise responses for cyanoacrylate in inclined planar cracks are given in Fig. 9. Crack inclination angles were between 77 and 82° measured from the horizontal. It can be noted

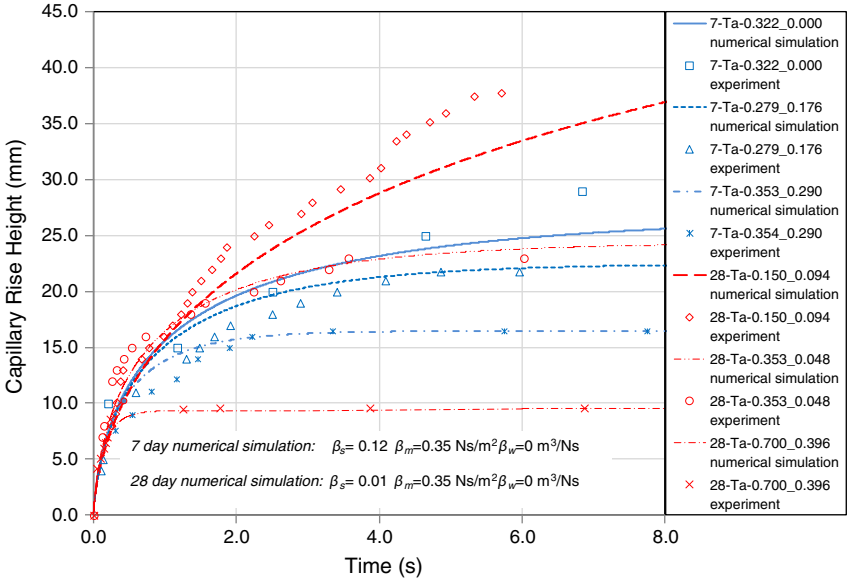

Fig. 10. Tapered crack capillary rise response for 7 and 28 day old specimens.

here that the shape of the response curve, together with the response times, are similar to those of the planar crack configuration, as predicted by the flow theory.

The tapered capillary rise response for a range of apertures is given in Fig. 10. It is difficult to draw comparisons between the 7 and 28 day results due to the different crack apertures employed, however, there is an indication that the initial capillary rise response of the 28 day old specimens is faster than that of the 7 day old specimens. This is contrary to previous observations made by Gardner et al. [16] and reflects the difference in the flow properties of water and cyanoacrylate and the interaction between the healing agent and the host matrix resulting in the retardation of the capillary rise response at younger specimen ages.

As observed in the planar and the inclined crack capillary rise responses, good agreement is obtained for the tapering cracks when β_s assumes the values of 0.12 and 0.01 for 7 and 28 day specimens respectively. Additionally, a β_m value of 0.35 Ns/m^2 was found to be appropriate for all crack apertures tested at all ages, reflecting the standardised surface roughness that was achieved in the specimen preparation prior to testing and confirming Blake's theory [26] that this correction parameter is constant for any particular combination of material and fluid considered. The β_w correction factor was set to 0 m^3/Ns in all cases, indicating no significant effect of wall slip on the capillary rise response of cyanoacrylate in discrete cracks in cementitious materials. This supports previous observations made by Gardner et al. [16] concerning the capillary flow of water in discrete cracks.

Whilst evidence of cyanoacrylate curing was not seen in the initial stages of the mortar channel experiments reported in Section 2, qualitative observations from the capillary rise experiments suggest that, 15 s after the start of the experiment, significant cyanoacrylate curing had occurred since it became difficult to separate the pair of specimens at that time. This is believed to be as a result of the low cyanoacrylate volume to contact surface area and smaller crack apertures which promoted bonding of the faces in the latter, in contrast to the higher cyanoacrylate volume to contact surface areas employed in the former.

6. Simulation of healing agent flow in a self-healing system

In this section the predictive capability of the capillary rise model for a healing agent in a real crack of known geometry will be assessed using data from tests undertaken at Cardiff University (Joseph at al. [11]). These experiments examined the efficacy of a self-healing cementitious system with embedded capillary tubes filled with cyanoacrylate, which ruptured upon damage and released cyanoacrylate into the crack plane. The extent of capillary flow during and after two loading cycles was recorded by the authors for a range of test variables. The healing agent used was an equivalent product to that employed in Section 3 and was supplied by four 3 mm inner diameter hollow capillary tubes, placed in a single layer, 20 mm from the bottom of the beam and open to the atmosphere at both ends, as indicated in Fig. 11 (a). All of the beams were subjected to two cycles of loading. In the first loading cycle the beam was loaded until it reached its initial peak value, at which point a sharp drop in the strength of the beam was recorded at the same time as a macro crack was observed to propagate from the underside of the beam. The test was then continued until the beam reached a crack mouth opening displacement (CMOD) of 0.3 mm, as measured by a clip gauge. At this point, the specimen was unloaded under stroke control, at the same constant rate used in the loading part of the cycle. After a 24 hour period the beams were re-tested to failure. A typical load-CMOD curve is presented in Fig. 11 (b) for the two loading cycles.

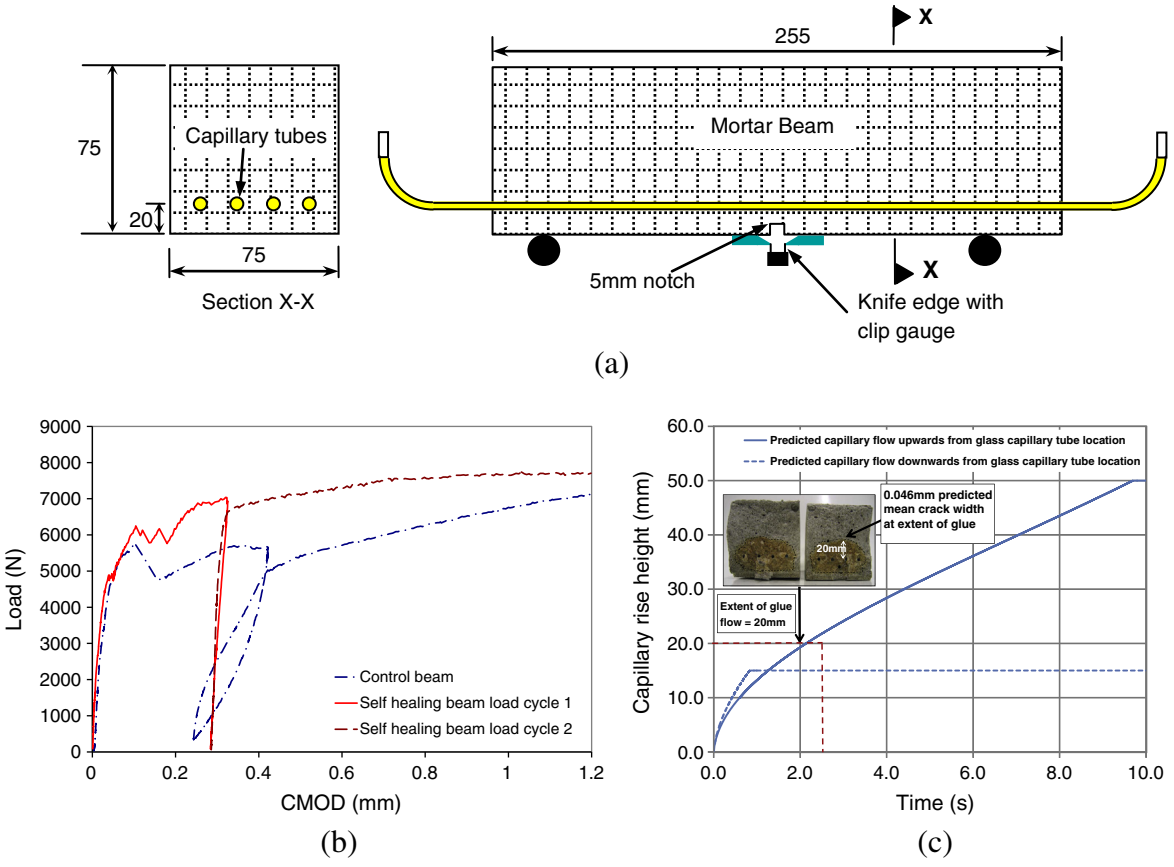

Fig. 11. (a) Self-healing experimental arrangement (b) load CMOD response of system (c) Predicted capillary rise response of self-healing system.

The CMOD value at which the first glass tube ruptured was noted during the experiments and in all cases this occurred at a CMOD value of 0.1 mm ± 0.015 mm. It is therefore assumed that the cyanoacrylate is released at a clip gauge CMOD of 0.1 mm. An assessment of the crack geometry at this CMOD value gives an opening of 0.077 mm at the level of the glass tubes and 0.0 mm 5 mm from the top of the specimen. This tapering crack profile yields the "upward" capillary rise response as observed in Fig. 11 (c). The "downward" capillary rise response concerns the profile of the crack from the level of the glass tubes (0.077 mm) to the tip of the notch (0.1 mm) and the prediction is based on gravity contributing to, rather than resisting, capillary flow. Although the capillary rise response is not visible during the tests, an indication of the extent of cyanoacrylate flow can be seen from the limit of cyanoacrylate flow observed in the specimens after failure, as given by the dashed line in Fig. 11(c). This final capillary rise was approximately 20 mm above the level of the glass capillary tubes. The prediction suggests that this would happen within 2.14 s of tube rupture, which would have allowed sufficient time for the cyanoacrylate to flow before curing started (in a crack of width 0.077 mm). Similarly the cyanoacrylate reaches the base of the crack within 0.84 s, and visual observations of fluid flowing from underneath the specimen moments after the breaking of the glass capillary tubes confirms this.

Without curing, the capillary rise would have been expected to reach (or almost reach) the top of the crack. However, as reported earlier in this paper, this cyanoacrylate is known to cure rapidly in gaps of 0.05 mm and less, and therefore the capillary rise would have been expected to arrest soon after reaching this crack opening. This was indeed the case, with the mean opening of the crack at the measured maximum rise height being 0.046 mm. It is noted that real flow path was tortuous and that the crack openings given are mean values. However, a previous study by the authors [16] on capillary flow of water in natural cracks suggests that it is reasonable to consider mean openings, which are equivalent to planar crack openings.

Whilst this assessment of the flow theory is not comprehensive, it does provide an indication of the applicability of the methods proposed to real self-healing systems.

7. Conclusions

The experimental arrangement used in this study allowed the capillary rise response of cyanoacrylate in a range of crack configurations and apertures to be measured. Planar, inclined and tapered crack configurations were all considered as well as the effect of specimen age on the shape and height of the capillary rise response.

In order to correctly model the rate of capillary rise, the time dependent properties of the cyanoacrylate were investigated. It was evident that the viscosity of the cyanoacrylate remained unchanged over a time period of 15 min for the capillary diameters used. However, there was evidence of cyanoacrylate curing over prolonged time periods (>2 h) as a result of either contamination with cementitious material or exposure to the atmosphere.

The experimental capillary rise response of cyanoacrylate in discrete cracks demonstrated that 28 day specimens always reached the theoretical equilibrium capillary rise height as suggested by the numerical solution using a β_s correction parameter of 0.01. The 7 day specimens consistently achieved lower equilibrium rise heights than those predicted by the numerical solution. It is suggested that this may be due to an interaction, in the presence of moisture and an alkaline environment, between the cyanoacrylate and the cementitious matrix, resulting in a retardation of the fluid front and subsequent stick slip behaviour.

Although equilibrium capillary rise heights in agreement with the modified Young–Laplace equation were observed for the planar and inclined crack configurations, the shape of the capillary rise response was different from that predicted by the standard L–W equation. Three correction factors, previously presented in the literature [16] were adopted in the numerical simulations presented in Section 6. For the capillary flow of cyanoacrylate in discrete cracks in mortar the correction parameter for stick-slip behaviour at the meniscus front (β_s) lies within the range of 0.12 to 0.01 for 7 to 28 day specimens respectively whilst the correction parameter for frictional dissipation at the meniscus wall (β_m) was 0.35 Ns/m^2 for both 7 and 28 day specimens. Previous studies with water placed the β_m correction value at 0.55 Ns/m^2 for 28 day specimens, confirming the unique relationship that exists for a particular combination of material and capillary fluid [16]. The correction parameter incorporating the slip between the fluid and solid wall (β_w) was 0 m^3/Ns in all cases which suggests that there is no significant influence of wall slip on the capillary rise response.

The application of the numerical model developed in this study to a self-healing specimen, tested in Cardiff, suggests that it is appropriate to use the model to predict the behaviour of such systems, provided that the rapid cyanoacrylate curing that occurs in openings below 0.05 mm is taken into account.

Acknowledgements

The authors acknowledge the financial support of the Engineering and Physical Sciences Research Council (EPSRC) under grant EP/J021776/1: *Capillary flow of autogenic and autonomic healing agents in discrete cracks in cementitious materials* and the loan of the Photron DVR High Speed Camera from the EPSRC Engineering Instrument Pool.

References

[1] V.C. Li, E. Herbert, Robust self-healing concrete for sustainable infrastructure, J. Adv. Concr. Technol. (6) (2012) 207–218.
[2] In: S. van der Zwaag (Ed.), An Alternative Approach to 20 Centuries of Materials Science, Springer, Dordrecht, The Netherlands, 2007.
[3] C. Joseph, D. Gardner, T. Jefferson, B. Isaacs, B. Lark, Self-healing cementitious materials: a review of recent work, Proc. Inst. Civ. Eng. Constr. Mater. 164 (1) (2010) 29–41.
[4] N. Hearn, Self-sealing, autogenous healing and continued hydration: what is the difference? Mater. Struct. 31 (8) (1998) 563–567.
[5] E. Schlangen, M. de Rooij, RILEM Technical Committee 221-SHC self-healing phenomena in cement-based materials, Draft of the State-of-the-Art Report2009.
[6] N. Ter Heide, E. Schlangen, K. van Breugel, Experimental study of crack healing of early age cracks, Proceedings of Knud Højgaard conference on Advanced Cement-Based Materials, Technical University of Denmark, June 2005.
[7] S.K. Ghosh, Self-healing Materials: Fundamentals, Design Strategies, and Applications, Wiley-VCH, Weinheim, Germany, 2009.
[8] C.M. Dry, Matrix cracking repair and filling using active and passive modes for smart timed release of chemicals from fibres into cement matrices, Smart Mater. Struct. 3 (2) (1994) 118–123.
[9] H. Mihashi, Y. Kaneko, T. Nishiwaki, K. Otsuka, Fundamental study on development of intelligent concrete characterized by self-healing capability for strength, Trans. Jpn Concr. Inst. 22 (2000) 441–450.
[10] V.C. Li, L. Yun Mook, C. Yin-Wen, Feasibility study of a passive smart self-healing cementitious composite, Compos. B: Eng. 29 (6) (1998) 819–827.
[11] C. Joseph, A.D. Jefferson, B. Isaacs, R.J. Lark, Experimental investigation of adhesive-based self-healing of cementitious materials, Mag. Concr. Res. 62 (11) (2010) 831–843.
[12] K. Van Tittelboom, N. De Belie, D. Van Loo, P. Jacobs, Self-healing efficiency of cementitious materials containing tubular capsules filled with healing agent, Cem. Concr. Compos. 33 (4) (2011) 497–505.
[13] Science Daily. Self-healing concrete: research yields cost-effective system to extend life of structures, see http://www.sciencedaily.com/releases/2010/05/100524143421.htm(for further details, Accessed 04/09/2011).
[14] T. Nishiwaki, H. Mihashi, B.-K. Jang, K. Miura, Development of self-healing system for concrete with selective heating around crack, J. Adv. Concr. Technol. 4 (2) (2006) 267–275.
[15] K. Van Tittelboom, N. De Belie, F. Lehmann, C. Grosse, Acoustic emission analysis for the quantification of autonomous crack healing in concrete, Constr. Build. Mater. 28 (1) (2012) 333–341.
[16] D.R. Gardner, A.D. Jefferson, A. Hoffman, Investigation of capillary flow in discrete cracks in cementitious materials, Cem. Concr. Res. 42 (7) (2012) 972–981.
[17] J. Rethore, R. de Borst, M.A. Abellan, A two-scale model for fluid flow in an unsaturated porous medium with cohesive cracks, Comput. Mech. 42 (2008) 227–238.
[18] E. Schäffer, P. Wong, Dynamics of contact line pinning in capillary rise and fall, Phys. Rev. Lett. 80 (14) (1998) 3069–3072.
[19] A. Hamraoui, T. Nylander, Analytical approach for the Lucas–Washburn equation, J. Colloid Interface Sci. 250 (2) (2002) 415–421.
[20] G. Martic, J. Coninck, T.D. Blake, Influence of the dynamic contact angle on the characterization of porous media, J. Colloid Interface Sci. 263 (2003) 213–216.

[21] M. Mooney, Explicit formulations for slip and fluidity, J. Rheol. 2 (1931) 210–222.
[22] W.-B. Young, Analysis of capillary flows in non-uniform cross-sectional capillaries, Colloids Surf. A 234 (2004) 123–128.
[23] R.W. Zimmerman, D. Chen, N.G.W. Cook, The effect of contact area on the permeability of fractures, J. Hydrol. 139 (1992) 79–96.
[24] N. Fries, M. Dreyer, An analytic solution of capillary rise restrained by gravity, J. Colloid Interface Sci. 320 (2008) 259–263.
[25] Cyanotech PC20 technical data sheet, available from http://www.gluegunsdirect.com/pc20(Accessed 01/06/2012).
[26] T.D. Blake, in: J.C. Berg (Ed.), Wettability, Marcel Dekker, New York, 1993.